TECHNICAL PAPER

nature
precedings

Large-scale imaging of brain network activity from >10,000 neocortical cells

Shigehiro Namiki[1,2], Norio Matsuki[1] & Yuji Ikegaya[1,3]

Large-scale recording from populations of neurons is a promising strategy in the study of complex brain function. Here we introduce a simple optical technique that simultaneously probes the calcium activity of ~10,000 cells at the single cell resolution *in vitro*. We employed a combination of a low-magnification objective lens and an electron-multiplying charge-coupled device megapixel camera to achieve large-view-field and high-resolution imaging.

Simultaneous monitoring of a huge number of brain cells is considered one of the possbile breakthroughs in modern neuroscience. At present, however, the maximal number of measureable cells is limited up to about 10^3, although a few promissing methods have been developed, including extracellular multiunit recordings (Buzsáki, 2004). Given that mammalian brains may carry the total number of 10^9 – 10^{11} neurons, furhter scaling up of the multicell recordings is waited for.

Functional multineuron calcium imaging is a technique that optically probes action potentials of neuron populations *en masse* at the single cell resolution (Takahashi et al., 2007). As an action potential reliably elicits a rapid and transient calcium rise in the cell body, one can reconstruct the firing activity via recording the change in the somatic calcium fluorescence intensity of the neuron. The same experimental system is also applicable for monitoring glial calcium activity. We thus call this optical technique that images neuronal and glial activities all together "functional multicell calcium imaging (fMCI)". In recent years, fMCI achieved simultaneous recordings from more than 10^3 neurons and unveiled novel network phenomena, such as flash-like attractor dynamics (Cossart et al., 2003), repeatable synfire-chain modules (Ikegaya et al., 2004), and precise cellular architectures of visual cortex columns (Ohki et al., 2006). These state-of-the-art recording methods have been advancing our knowledge about how the brain network operates at a mesoscopic scale.

To gain the single cell resolution, these studies employed relatively high-magnification objective lens, such as 20× (Cossart et al., 2003; Kerr et al., 2005; Dombeck et al., 2007; Yaksi et al, 2007) and 40× (Ohki et al., 2006; Crépel et al., 2007). The use of high-magnification objectives limits the number of measureable cells to maximally about 10^3 and the size of the imaging field to about 500 × 500 μm^2. To cover wider areas, lower-magnificaiton objectives, such as 4×, are required, but they usually lack the cellular resolution and sufficient signal intensity in conventional experimental systems. Moreover, when they are combined with a photomultiplier tubes (PMTs), the acquisition rate is slowed, and the laser-dwell time period for each cell is shortened, resulting in a worse signal-to-noise (S/N) ratio. Alghouth arrayed PMTs are available, they do not at present attain a spatial resolution sufficient to isolate individual cells (Kim et al., 2007).

The single cell resolution has been attained by use of megapixel charge couple device (CCD) or complementary metal–oxide–semiconductor cameras (Bosiers et al., 2008), but the S/N is insufficent for the fMCI. This problem is solved herein with a high-sensitivity imaging system with an electron-multiplying (EM) CCD camera. In the present study, we combined a recently developed back-illuminated EM-CCD megapixel camera to a 4× low-magnification objective lens and succeeded in monitoring the calcium activity of a large number of cells in acute neocortical slices.

RESULTS

As the juvenile rodent neocortex, in general, has a high density of neurons, we imaged ~3 × 3-mm^2 area in acute neocortical slices of developing rats. In each movie, individual cells were semi-automatically detected. The total number of simultaneously monitored cells was, on average, 9,035 ± 2,063 cells (mean ± SD of 5 slices), ranging from 5,569 to 10,669 cells. A representative data, including 10,669 cells, is shown in **Figs. 1&2** and **Supplementary Movie** (http://neuronet.jp/data/large_scale_movie.mov).

We then reconstructed the time series of spontaneously occurring transient calcium events for each cell. Event times were automatically detected by thresholding the calcium trace at the 3 × standard

[1]Laboratory of Chemical Pharmacology, Graduate School of Pharmaceutical Sciences, The University of Tokyo, 7-3-1 Hongo, Bunkyo-ku, Tokyo 113-0033, Japan, [2]Graduate School of Life and Environmental Sciences, University of Tsukuba, 1-1-1 Tennodai, Tsukuba, Ibaraki 305-8572, Japan, [3]Precursory Research for Embryonic Science and Technology, Japan Science and Technology Agency, 5 Sanbancho Chiyoda-ku, Tokyo 102-00075, Japan. Correspondence should be addressed to YI (Ikegaya@mol.f.u-tokyo.ac.jp).

http://hdl.handle.net/10101/npre.2009.2893.1

Received 23 February 2008; Posted 23 February 2009

deviations of the background noise level and plotted in a rastergram form (**Fig. 3**).

The rastergram involves both neurons and non-neuronal cells (*e.g.*, glial cells), and both types of cells exhibited calcium activity. Thus we separated the cell types, based on their calcium dynamics; note that the kinetics of glial calcium events is usually more than 10-fold slower than that of neurons (Ikegaya et al., 2005). In Fig. 3, blue and red colors indicate the activity of putative neurons and glial cells, respectively. Inter-cellularly synchronized calcium events were observed only in putative neuron groups, suggesting that our automatic separation works to a considerable extent.

We also monitored the spontaneous activity in acute hippocampal slices. We were able to simultaneously monitor the network activity of the dentate gyrus, the CA3 region, and the CA1 region, including a few thousand of cells (n = 12 slices, data not shown).

DISCUSSION

There are two major advantages for this method in comparison with conventional fMCI, *i.e.*, measurable cell numbers and large fields of view.

As previously reported in Cossart et al. (2003), Ikegaya et al. (2004), and Ohki et al. (2006), fMCI has already succeeded in recording from more than 10^3 cells, but to our knowledge, our new technique is the first to monitor the activity from more than 10^4 cells. This imaging system uses a high-sensitivity camera that has more than 10^6 sensors and a spinning-disk confocal unit that rapidly scans the microscopic field by emitting about 2×10^4 laser beams at a moment, thus embodying such large-scale recordings with maintaining the single-cell resolution. Conventional raster scanning methods employ single point illumination and single point scanning, and thus, the resultant short-dwell time periods put restrictions on the number of measurable cells and the S/N, although it is somewhat improved by controlling the scanning path (Göbel et al., 2007; Lillis et al., 2008; Reddy et al., 2008).

Our method would be useful, in particular, to address spatially discrete networks, such as trisynaptic circuits in the hippocampus and relay circuits from thalamus to the somatosensory cortex, because the flow and processing of information can be directly accessed in real time in these networks.

The major drawback of this technique seems to be its relatively low S/N. This will be overcome by development of higher-performance optical sensors. Another disadvantage is the difficulty to indentify the cell types. EM-CCD multi-megapixel camera may help more accurate cell-type discriminations. Finally, in our large-scale fMCI, the huge data size makes it difficult to treat them manually. Thus, sophisticated data-processing software and supercomputer-based environments are both indispensable for practical use.

METHODS

Materials. Oregon Green BAPTA-1AM (OGB-1) and Pluronic F-127 were obtained from Invitrogen (Carlsbad, CA, USA). Cremophor EL was obtained from Sigma-Aldrich (St. Louis, MO, USA). The stock solutions were stored at –20°C and diluted immediately before use. All salts were obtained from Wako Chemicals (Osaka, Japan).

Acute brain slice preparations. According to the Japanese Pharmacological Society guide for the care and use of laboratory animals, postnatal 6-to-9-day-old rats (SLC, Shizuoka, Japan) were deeply anesthetized with ice and immediately decapitated. The brain was quickly removed (< 30 s) and immersed in ice-cold modified artificial cerebrospinal fluid (ACSF) consisting of (in mM) 27 $NaHCO_3$, 1.4 NaH_2PO_4, 2.5 KCl, 0.5 ascorbic acid, 7.0 $MgSO_4$, 1.0 $CaCl_2$, and 222.1 sucrose. ACSF was continuously bubbled with 95% O_2 and 5% CO_2. The leptomeninx was carefully removed by a pair of sharp forceps. This procedure is required to make the slice surfaces flattened, thus being critical for wide view-field recording. Horizontal slices at 400 µm in thickness were prepared using a microslicer (Vibratome 3000; Vibratome Company, St. Louis, MO, USA). The same surface of the slice was kept at the upper side throughout the experiments. After dissection, slices were maintained for 30 min at room temperature in ACSF, consisting of (in mM): 127 NaCl, 26 $NaHCO_3$, 1.5 KCl, 1.24 KH_2PO_4, 1.4 $MgSO_4$, 2.0 $CaCl_2$ and 10 glucose.

Calcium indicator loading. OGB-1 was selected to visualize calcium signal because of three following reasons; (1) relatively excellent efficiency of dye loading into neurons, (2) high S/N, and (3) appropriate dissociation constant (170 nM) to detect single action potentials. Slices were transferred into a multiwell plate (6-well Multiwell Plate; BD Bioscience, San Jose, CA, USA) filled with 4 ml of ACSF, and 5 µl of dye solution was directly applied to the slice surface. The dye solution consisted of 0.07% OGB-1, 1.4% Pluronic F-127, and 0.7% Cremophor EL in DMSO. The slices were incubated for 30 min at a room temperature in an incubation chamber (Ikegaya et al., 2005). After being washed, they were maintained in dye-free ACSF at room temperature for > 30 min.

Calcium imaging. A slice was transferred into a recording chamber and perfused with physiological ACSF consisting of (in mM): 127 NaCl, 26 $NaHCO_3$, 3.3 KCl, 1.24 KH_2PO_4, 1.0 $MgSO_4$, 1.0 $CaCl_2$ and 10 glucose, warmed at 30 – 32°C with a temperature controller (TC-344B; Warner Instruments Corporation, Hamden, CT, USA), at a flow rate of 1.0 – 2.0 ml/min. After > 15 min of perfusion, spontaneous calcium signals were recorded. Movies (1,024 × 1,024 pixels, 12-bit intensity) were captured at 1 – 4 frame/s with a CSU-22 confocal scanner unit (Yokogawa Electric, Tokyo, Japan), cooled EM-CCD camera (iXon EM^+ DU888DCS-BV; Andor Technology, Belfast, UK), a Nikon Eclipse FN-1 upright microscope (Tokyo, Japan), a 4× dry objective lens with 0.20 numerical aperture (CFI Plan Apochromat, Nikon), and SOLIS image acquisition software (Andor Technology). The top of the recording chamber was sealed with a 22 × 22-mm^2 coverslip (thickness, 0.12 – 0.17 mm; Matsunami Glass, Osaka, Japan) to reduce the water-level fluctuations that caused photo-scattering and image deformation. OGB-1 was excited at 488 nm with an argon-krypton laser (10 – 20 mW, 641-YB-A01; Melles Griot, Carlsbad, CA, USA) and visualized through a 507-nm long-pass emission filter. A custom-made optical relay-lens adaptor was inserted between the confocal unit and the CCD camera to adjust the image size emitted from CSU22 to the CCD array size (13.3 × 13.3 mm). As a result, the microscopic field of 3,250 × 3,250 μm^2 was captured at a pixel size of 3.17 µm.

Data analysis. The regions of interest (ROIs) were automatically detected with a custom-made program (Cossart et al., 2003). The ROIs with the area of < 70 μm^2 were discarded. The other false detection was manually corrected. The fluorescence intensity of individual pixels within a single ROI was averaged and time series of the intensity were calculated. For each cell, the fluorescence change was calculated as $(F_t - F_0) / F_0$, where F_t is the fluorescence intensity at any time point, and F_0 is the average signal intensity during the baseline period. All programs were written in MATLAB (Mathworks, Natick, MA, USA).

ACKNOWLEDGEMENTS

We are grateful to Masatoshi Yaji (Andor Technology) and Tadayoshi

Ogura (Nikon Instruments) for their comments on the experimental system, and Takuya Sasaki for his suggestions on the manuscript. This work was supported in part by a Grant-in-Aid for Science Research on Priority Areas (Elucidation of neural network function in the brain: KAKENHI#20019014), a Grant-in-Aid for Science Research (KAKENHI# 19659013), and the Supercomputing Division in the Information Technology Center at the University of Tokyo.

Bosiers, J. T. *et al*. Challenges and innovations in very-large CCD and CMOS imagers for professional imaging. *Proc. SPIE* **6996,** 69960Z (2008).

Buzsáki, G. Large-scale recording of neuronal ensembles. *Nat Neurosci* **7,** 446-451 (2004).

Cossart, R., Aronov, D., & Yuste, R. Attractor dynamics of network UP states in the neocortex. *Nature* **423,** 283-288 (2003).

Crépel, V. *et al*. A parturition-associated nonsynaptic coherent activity pattern in the developing hippocampus. *Neuron* **54,** 105-120 (2007).

Dombeck, D. A., Khabbaz, A. N., Collman, F., Adelman, T. L., & Tank, D. W. Imaging large-scale neural activity with cellular resolution in awake, mobile mice. *Neuron* **56,** 43-57 (2007).

Göbel, W., Kampa, B. M., & Helmchen, F. Imaging cellular network dynamics in three dimensions using fast 3D laser scanning. *Nat Methods* **4,** 73-79 (2007).

Ikegaya, Y. *et al*. Synfire chains and cortical songs: temporal modules of cortical activity. *Science* **304,** 559-564 (2004).

Ikegaya, Y., Le Bon-Jego, M. & Yuste, R. Large-scale imaging of cortical network activity with calcium indicators. *Neurosci Res* **52,** 132-138 (2005).

Kerr, J. N. D., Greenberg, D., & Helmchen, F. Imaging input and output of neocortical networks *in vivo*. *Proc Natl Acad Sci U S A* **102,** 14063-14068 (2005).

Kim, K. H. *et al*. Multifocal multiphoton microscopy based on multianode photomultiplier tubes. *Opt Exp* **15,** 11658-11678 (2007).

Lillis, K. P., Eng, A., White, J. A., & Mertz, J. Two-photon imaging of spatially extended neuronal network dynamics with high temporal resolution. *J Neurosci Methods* **172,** 178-184 (2008).

Ohki, K. *et al*. Highly ordered arrangement of single neurons in orientation pinwheels. *Nature* **442,** 925-928 (2006).

Reddy, G. D., Kelleher, K., Fink, R., & Saggau, P. Three-dimensional random access multiphoton microscopy for functional imaging of neuronal activity. *Nat Neurosci* **11,** 713-720 (2008).

Takahashi, N., Sasaki, T., Usami, A., Matsuki, N., & Ikegaya, Y. Watching neuronal circuit dynamics through functional multineuron calcium imaging (fMCI). *Neurosci Res* **58,** 219-225 (2007).

Yaksi, E., Judkewitz, B., & Friedrich, R. W. Topological reorganization of odor representations in the olfactory bulb. *PLoS Biol* **5,** e178 (2007).

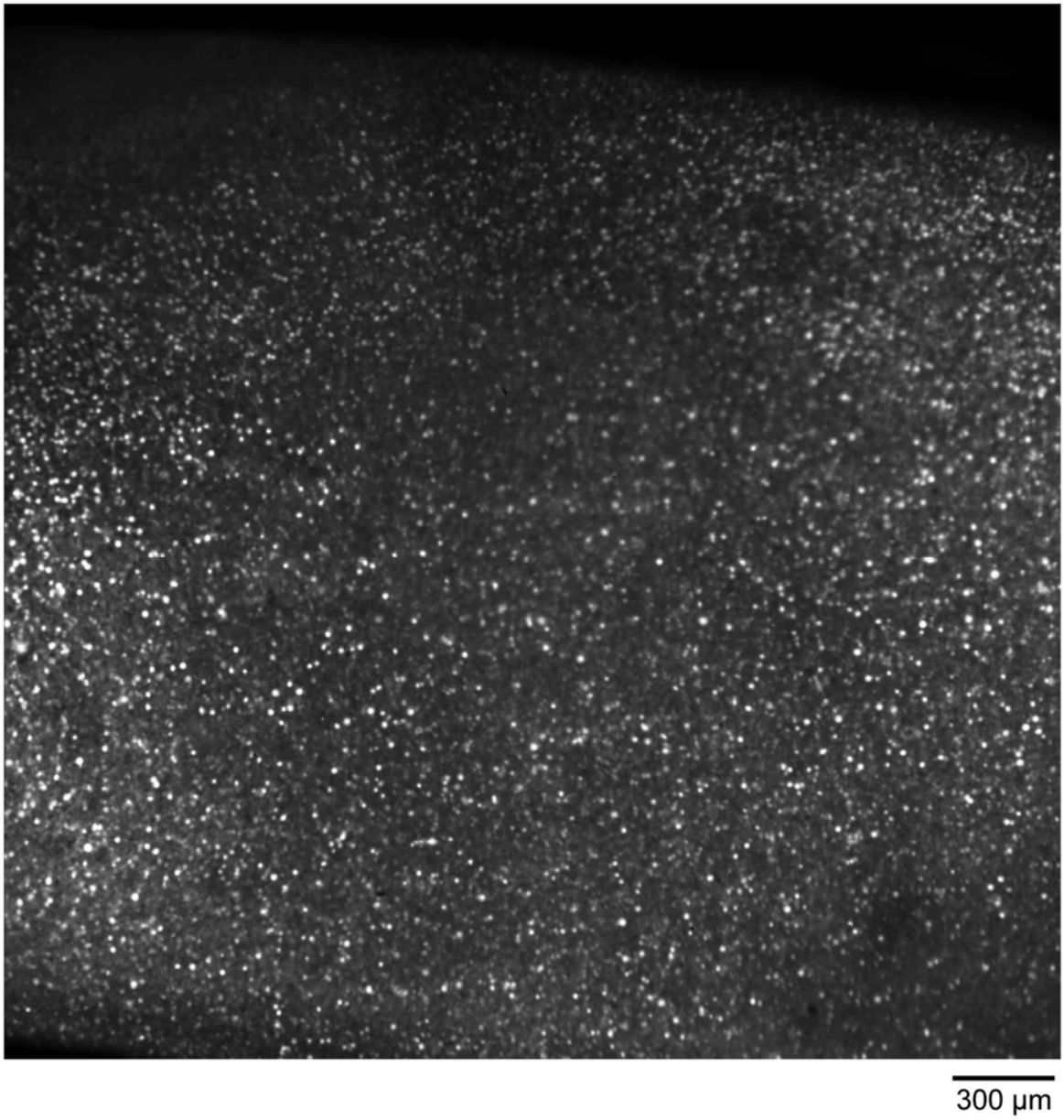

Figure 1 Representative single frame in a movie taken from a rat motor cortex slice loaded with OGB-1. The view field is 3,250 µm × 3,250 µm, covering the layer I to VI, in which 10,669 cells are indentified by an automatic detection algorithm. A part of the original movie is available online at http://neuronet.jp/data/large_scale_movie.mov.

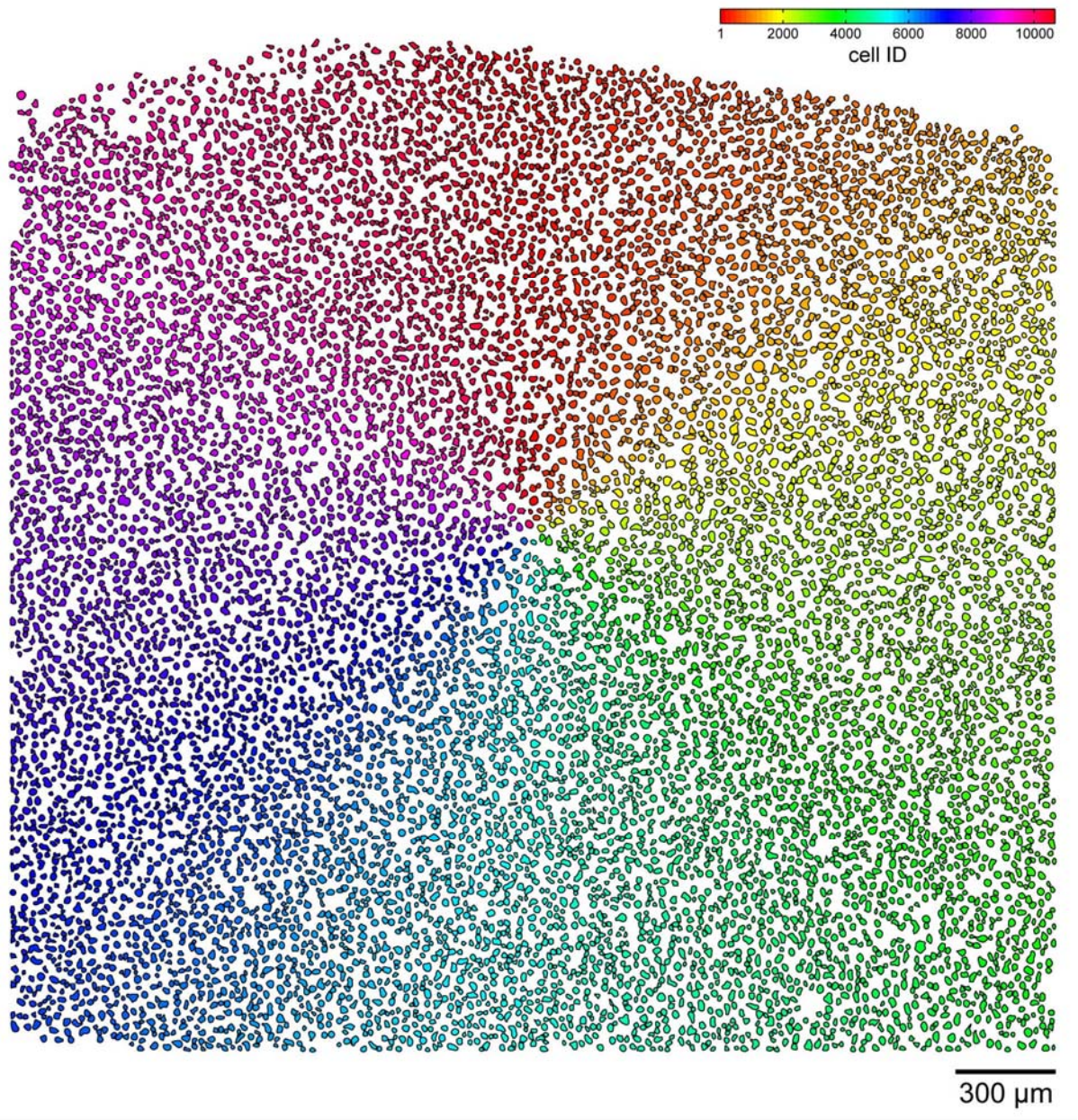

Figure 2 Cell map reconstructed from the movie of Figure 1. Cells are arbitrarily assigned serial ID numbers from 1 to 10,669, which are indicated in a pseudo-color scale.

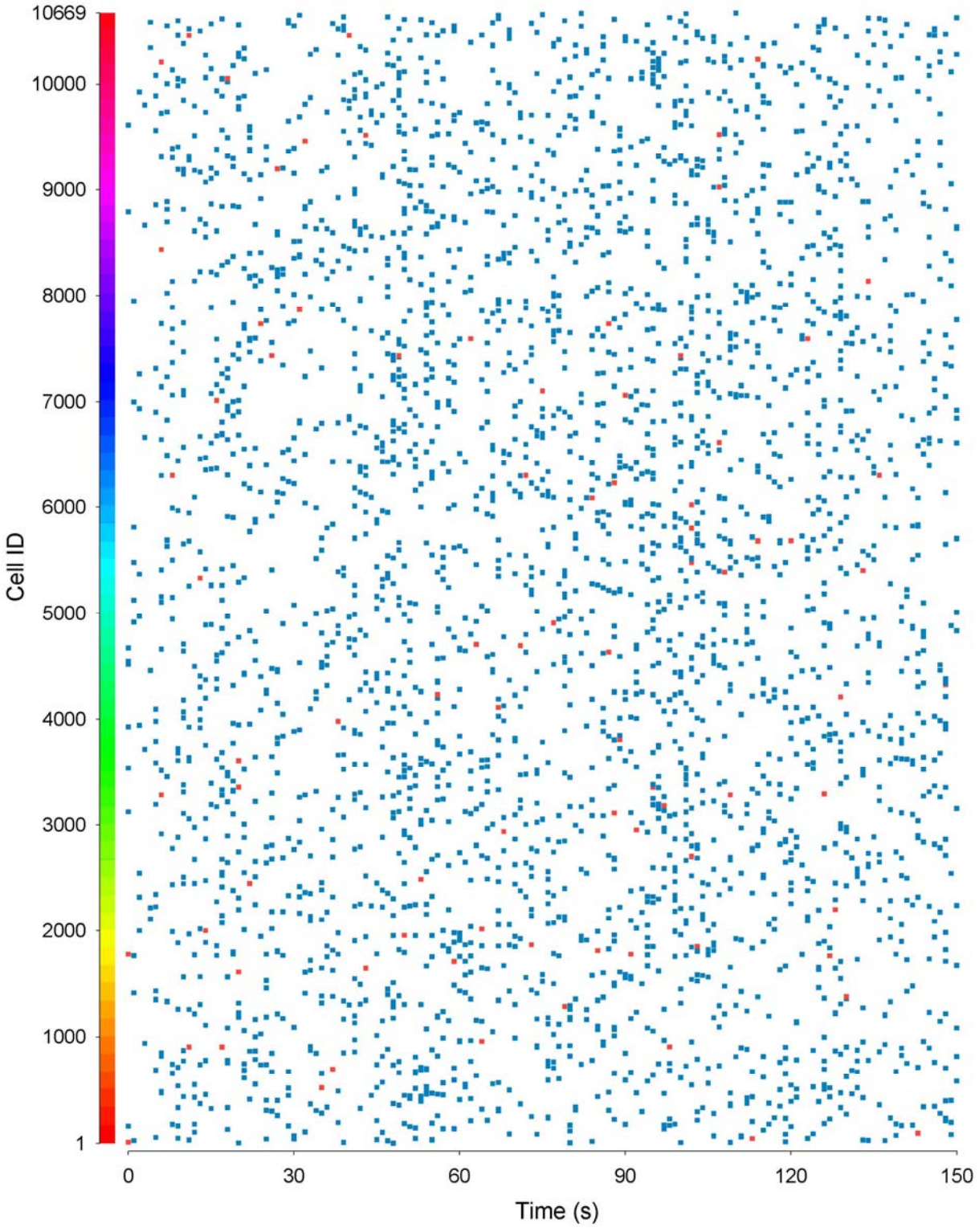

Figure 3 Rasterplot of the calcium activity exhibited by 10,669 cells in the movie of Figure 1. The pseudo-color scale of the cell ID number on the Y axis corresponds to that in Figure 2. Each dot represents the timing of a single calcium event. Blue and red dots are signals of putative neurons and glial cells, respectively.